Available online at www.sciencedirect.com
SCIENCE DIRECT
ELSEVIER
International Journal of Pharmaceutics 313 (2006) 99–113
INTERNATIONAL JOURNAL OF PHARMACEUTICS
www.elsevier.com/locate/ijpharm

Rapid determination of dry layer mass transfer resistance for various pharmaceutical formulations during primary drying using product temperature profiles

Wei Y. Kuu [a,*], Lisa M. Hardwick [b], Michael J. Akers [b]

[a] *BioPharma Solutions, Baxter Healthcare Corporation, Round Lake, IL 60073, United States*
[b] *BioPharma Solutions, Baxter Healthcare Corporation, Bloomington, IN 47403, United States*

Received 18 June 2005; received in revised form 1 November 2005; accepted 19 January 2006
Available online 28 February 2006

Abstract

Mass transfer resistance of the dry layer during the primary drying phase of a lyophilizaton cycle is probably the most important factor affecting maximum product temperature and drying time. Product resistance parameters should be determined for each formulation because of their dependence of formulation composition and concentration. The purpose of this study was to determine the dry layer mass transfer resistance, using a simple and rapid method, for various pharmaceutical formulations during primary drying in a laboratory dryer, using monitored product temperature profiles. The mathematical tools used for the determination were a primary drying simulation program in conjunction with Powell's optimization algorithm. For each formulation studied, primary drying was performed using a shelf temperature of −15 or −20 °C and the chamber pressure controlled at 100 mTorr (0.1 Torr). The product temperature profiles (T_b) during primary drying were recorded and became the input data for the parameter estimation. The normalized product resistance, R_{pN}, as a function of the dry layer thickness, ℓ, can be described by: $R_{pN} = R_0 + A_1\ell/(1 + A_2\ell)$, where the constants R_0, A_1 and A_2 are product resistance parameters of water vapor through the dry layer. Even when the parameter A_1 was negative, indicating that product temperature atypically decreased over time, the dry layer product resistance parameters of the various pharmaceutical formulations could be rapidly and successfully determined using the proposed approach. The product resistance equation obtained in this work for 5% marmitol, expressed as $R_{pN} = 0.0002025 + 20.23\ell$, is similar to that obtained by Pikal [Pikal, M.J., 1985. Use of laboratory data in freeze drying process design: heat and product resistance parameters and the compute simulation of freeze drying. J. Parent. Sci. Technol. 39, 115–138.] using the microbalance method, expressed as $R_{pN} = 1.40 + 16.0\ell$. The product resistance values obtained for the 3% lactose–LDH formulation are also very close to those obtained by (Milton, N., Pikal, M.J., Roy, M.L., Nail, S.L., 1997. Evaluation of manometric temperature measurement as a method of monitoring product temperature during lyophilization. PDA J. Pharm. Sci. Technol. 51, 7–16.) for 5% lactose using the MTM (manometric temperature measurement) method. With the obtained values of the parameters R_0, A_1, and A_2, simulations can be performed to determine the maximum product temperature and the drying time during primary drying. As such, optimum cycle parameters can be determined to avoid collapse of the product. The proposed approach requires only accurately measured product temperature profiles, easily obtained in a laboratory dryer.

Keywords: Collapse temperature; Dry layer product resistance parameters; FORTRAN; Lactose dehydrogenase (LDH); 5% Mannitol; Mass transfer resistance; Micro-collapse; Newton–Ralphson iteration; Powell's optimization algorithm; Primary drying; Primary drying subroutine

1. Introduction

One of most important issues associated with freeze-drying of pharmaceuticals is collapse of the product during primary drying, as the result of the product temperature exceeding the collapse temperature (or eutectic temperature for compounds that form crystallines after freezing, Pikal, 1985). The primary drying process is governed by at least six heat transfer processes and two mass transfer processes described below. If trays are used, the heat transfer processes include the following routes: (1) from the shelf fluid to the shelf surface, (2) from the shelf surface to the tray, (3) from the tray surface to the bottom of the glass vial through thermal conduction of glass, (4) from the tray surface to the bottom of the vial through thermal conduction of

* Corresponding author. Tel.: +1 847 270 5974; fax: +1 847 270 5999.
E-mail address: wei_kuu@baxter.com (W.Y. Kuu).

0378-5173/$ – see front matter © 2006 Elsevier B.V. All rights reserved.
doi:10.1016/j.ijpharm.2006.01.036

Nomenclature

a_c	the energy accommodation coefficient of the gas
ASV	the shelf area per vial (cm^2)
ATV	the tray area per vial (cm^2)
A_p	cross-sectional area of the product in the vial (cm^2)
A_v	vial area (calculated based on the outside diameter) (cm^2)
A_1 and A_2	product resistance parameter, used in Eq. (1)
d	inside diameter of the vial (cm)
dm/dt	sublimation rate (g/h)
e_s	emissivity of the shelf surface thermal radiation (dimensionless)
e_v	emissivity of the vial top thermal radiation (dimensionless)
KC, KD	constants associated with vial heat transfer coefficient K_v. KC = $K_{cs} + K_r$, and KD = $\ell_v(\alpha\Lambda_0/\lambda_0)$. For Wheaton 10 mL tubing vial, KC = 2.64×10^{-4} and KD = 3.64 (Pikal, 1985)
KP	constant associated with vial heat transfer coefficient, KP = $\alpha\Lambda_0$. The value of KP is equal to 3.32×10^{-3}, obtained by Pikal (1985) for all vials tested
KTC	the sum of radiative and contact terms of the tray heat transfer
KTD	equal to $\ell_T(\alpha\Lambda_0/\lambda_0)$, where ℓ_T is the mean separation distance between the tray bottom and the shelf surface
KTP	equal to $\alpha\Lambda_0$ for the tray
K_g	gas heat transfer coefficient (cal s^{-1} cm^{-2} $°C^{-1}$)
K_I	effective thermal conductivity of the frozen layer (cal s^{-1} cm^{-1} $°C^{-1}$)
K_s	shelf surface heat transfer coefficient (cal s^{-1} cm^{-2} $°C^{-1}$)
K_{tr}	tray heat transfer coefficient (cal s^{-1} cm^{-2} $°C^{-1}$) K_{tr} = KTC + KTP P/(1 + KTD P)
K_v	vial heat transfer coefficient (cal s^{-1} cm^{-2} $°C^{-1}$)
ℓ	thickness of the dry layer at any time (cm)
ℓ_m	maximum thickness of the frozen layer (cm)
ℓ_v	separation distance of the vial (cm)
m_{avg}	the average rate of sublimation (g/h)
P_c	chamber pressure (mmHg)
P_v	pressure in the vial (mmHg)
P_0	equilibrium vapor pressure of the subliming ice (mmHg)
Q	rate of heat transfer (cal s^{-1})
R_p	dry layer resistance (Torr h g^{-1})
R_{pN}	area normalized dry layer resistance (cm^2 Torr h g^{-1})
R_s	stopper resistance (Torr h g^{-1})
R_0	product resistance parameter product resistance parameter, used in Eq. (1)
SSQ	sum of squares
S_0, S_1	stopper mass transfer constants
T_b	temperature at the bottom-center of the frozen layer (K)
T_f	temperature of the cooling fluid in the freeze dryer (K)
T_i	temperature at the moving surface of the frozen solution (K)
T_s	shelf temperature (K)
T_t	surface temperature of the tray (K)

Greek letters

α	defined by Eq. (6)
λ_0	thermal conductivity of gas at ambient temperature, equal to 4.29×10^{-5} (cal s^{-1} $°C^{-1}$ cm^{-1})
ρ	density of frozen layer (g cm^3)
σ	Stefan–Boltzmann constant, equal to 1.35×10^{-12} (cal cm^{-2} s^{-1} K^{-4})
Λ_0	free molecular heat conductivity of water at 0 °C, equal to 6.33×10^{-3} (cal s^{-1} cm^{-2} K^{-1} $mmHg^{-1}$)

gas, (5) from the overhead shelf bottom to the vial top surface, and (6) thermal conduction through the frozen layer. If no tray is used, step 2 can be omitted and the "tray surface" in steps 3 and 4 should be replaced by "shelf surface." The two mass transfer processes include: (1) permeation of water vapor through the dry product layer, and (2) escaping of water vapor through the stopper vent. Among the above processes, only the mass transfer resistance is specific to the formulation. Other processes are associated with the characteristics of the dryer, the vial, the stopper, and the frozen ice layer. The heat transfer parameters for these processes are either available or can be determined independently using relatively simple experiments. These parameters will not change as long as the same dryer, vial and stopper are used for freeze-drying.

By comparison, determination of product resistance parameters is much more complicated. Conventional ways of determination require a gravitational method to monitor the weight loss of samples at various time intervals (Pikal et al., 1983). One of the issues associated with microbalance use is that the sample cannot be made to freeze as does a sample in a vial. Because ice crystal size determines resistance and super-cooling determines ice crystal size, any method for determining resistance must be capable of approximating the super-cooling characteristic of the process of interest.

Another novel approach, developed recently, is called the manometric temperature measurement (MTM) method (Milton et al., 1997; Tang et al., 2005). It is a procedure to measure the product temperature during primary drying by quickly isolating the freeze-drying chamber from the condenser and analyzing the pressure rise during this period. The "pressure rise" approach is a novel approach for monitoring the product temperature of the cycle run, and an excellent method for process development, because of its non-invasive nature. However, there are several limitations if it is used for determination of the product resis-

tance. As pointed out by Tang et al. (2005, page 689), the number of vials still containing ice must remain appreciable for the batch during the pressure rise measurement. Otherwise the value of R_{pN} is no longer accurate. For example, the obtained resistance is no longer accurate after about 60% of total primary drying time for 5% sucrose and at about 80% of total primary drying time for 5% glycine. The problem is more severe when the primary drying is conducted at low shelf temperature, and for a low dry layer resistance product such as 5% sucrose. As a general rule, the MTM determined resistance is valid until about 2/3 of total primary drying time has expired.

Another obvious advantage of the proposed approach in this paper is that the product resistance of multiple formulations can be determined simultaneously without interruption of the cycle run. As long as at least one vial for each formulation can be probed with thermocouple, the number of formulations in any study cycle is limited only by the available number of thermocouples in the dryer.

1.1. The rationale

During a set freeze-drying cycle, the only variables that can be continuously monitored and recorded without disturbing the vials on the shelf are the temperature (including the temperature of the product, shelf fluid, and shelf surface) and the chamber pressure. After the ramping period of primary drying, the pressure profiles usually do not vary significantly from the setpoints, and have no clear trend during sublimation. Therefore, there is no meaningful correlation between the progress of sublimation and the pressures. The only useful data are the: product temperature profiles.

The rationale of using the product temperature profiles to determine the dry layer product resistance parameters is discussed below. The product temperature during the course of primary drying is the consequence of heat and mass transfers into and out of the vial and the sublimation cooling of the frozen formulation. As such, usually the product temperature will vary during primary drying with a predictable trend, and can be recorded over time. The method for predicting the product temperature is by combining the heat and mass transfer mechanisms (Pikal, 1985; Pikal et al., 1984) and solving these equations simultaneously. In order to use the measured product temperature profiles to determine the product resistance parameters, it requires a parameter estimation algorithm.

1.2. Requirements for determination of product resistance parameters

The requirements for determination of product resistance parameters, using the product temperature profiles, include the following three items. First, it is necessary to develop a simulation program for primary drying by combining the heat and mass transfer mechanisms of primary drying. The FORTRAN source code developed for this purpose is called primary drying subroutine PDRYS in this paper. Second, it is essential to develop a computation algorithm that is capable of performing a "regression" analysis to search for the "best-fit" parameters. The algorithm used in this paper is Powell's nonlinear parameter estimation technique (Powell, 1965; Himmelblau, 1972; Kuester and Mize, 1973; Kuu et al., 1992, 1995). The detailed computation procedure is discussed later in this paper. The third requirement is accurately measured product temperature profiles during primary drying. This information is usually obtained during the cycle run using a laboratory dryer. Therefore, no additional tedious experiments are required.

The purpose of this paper is to perform a rapid determination of dry layer product resistance parameters for various pharmaceutical formulations during primary freeze-drying using monitored product temperature profiles. The resulting parameters can then be used for simulations to: (1) determine the product temperature profiles T_b during the primary drying to ensure that the T_b is below the collapse temperature, (2) estimate the drying time of primary drying, and (3) establish a correlation between the laboratory and production dryers.

2. Theoretical background of primary drying

The heat and mass transfer processes involved in primary drying of pharmaceuticals have been extensively investigated by a number of researchers (Dyer and Sunderland, 1968; Karel, 1975; Mellor, 1978; Ho and Roseman, 1979; Nail, 1980; Pikal et al., 1984; Millman et al., 1985; Pikal, 1985; Lombrana and Diaz, 1987; Jennings, 1988). Among them, one of the most thorough analyses was attributed to Pikal (1985) who developed a mathematical model to combine all processes in primary drying from the shelf to the condenser. The theoretical foundation of primary drying was established by Pikal et al. (1984) and Pikal (1985). The physical model is depicted in Fig. 1 of Pikal (1985), where the primary drying process is governed by the complex heat and mass transfer mechanisms through the vial, as depicted in Fig. 1 of the literature (Pikal, 1985). To simplify the mechanisms, it is assumed that the heat and mass transfer processes are one-dimensional and vary only in the vertical direction. This may be achieved by thermal shielding from adjacent vials or, for a research purpose, by insulating the side walls of the vials. As scon as the thermal equilibrium is reached, it is reasonable to assume that a pseudo-steady state is established within a small time interval of sublimation. This assumption includes two implications. First, the rate of heat transfer across the various phases, from the shelf to the surface of the frozen layer, is constant. Second, the temperature profile is linear across the frozen layer at any drying time during primary drying.

In the sublimation process, the product temperature becomes a function of the sublimation rate, the geometry and configuration of the vial, the thickness of the frozen product in the vial, the chamber pressure, and the mass transfer resistance of the dry layer. The dry layer resistance is particularly important for a solution with a relatively large fill depth. It gradually increases during the drying period, resulting in increasing of the mass transfer resistance through the dry layer, followed by warming of the frozen layer. As such, a desired beginning temperature of the frozen layer does not always warrant a successful primary drying throughout the entire period.

Under an isothermal condition, the mass transfer resistance may be directly determined by experiments, such as the freeze-drying microbalance technology used by Pikal et al. (1983), where the dried layer resistances of a number of formulations under various thermal histories have been obtained using this method. A sophisticated freeze-drying microbalance, however, is needed to perform this task. The approach proposed in this paper intends to minimize experimental efforts. It will be shown later that the parameter estimation approach proposed in this work does not require an isothermal condition. In the computation procedure, the ice temperature at the receding surface of the frozen layer T_i is automatically computed using the heat and mass transfer equations for each time interval.

2.1. Equations of heat and mass transfer

The equations of heat and mass transfer mechanisms used in this paper are obtained from Pikal (1985, Eqs. (2), (3), (12), (15), (18), (22)–(26), (28), (29), (31), (32) and (41)). The heat transfer rate around the vial Q is the most complicated item. It includes the following routes: (1) direct conduction from the shelf to the glass vial at the point of contact, (2) radiative heat transfer from the shelf surface to the vial bottom, and (3) conduction of gas between the shelf and vial bottom, and (4) radiative heat transfer from the overhead shelf bottom to the vial top. Q can be expressed by the following equation (Pikal et al., 1984, modified from Eq. (19) of the literature, without using the simplified Eq. (4) in this paper):

$$Q = A_v(K_{cs} + K_g)(T_t - T_b) + A_v e_s \sigma(T_t^4 - T_b^4) + A_v e_v \sigma(T_s^4 - T_i^4) \quad (1)$$

where σ is the Stefan–Boltzmann constant, equal to 4.86×10^{-9} cal cm^{-2} h^{-1} K^{-4} or 1.35×10^{-12} cal cm^{-2} s^{-1} K^{-4}. K_{cs} is the conductive heat transfer parameter of the contact point between the shelf and glass vial (the contact parameter), A_v the vial area (calculated based on the outside diameter), T_t the tray temperature, T_b the temperature at the bottom of the frozen layer, and T_i is the temperature at the ice sublimation surface.

Since Eq. (1) is highly nonlinear, Pikal et al. (1984) and Pikal (1985) used the following simplified equation:

$$Q = A_v K_v (T_t - T_b) \quad (2)$$

where the vial heat transfer coefficient K_v is the sum of three contributions:

$$K_v = K_{cs} + K_r + K_g \quad (3)$$

where K_r is the radiative heat transfer coefficient, and K_g is the conductive heat transfer coefficient of the gas between the shelf and the glass vial. The radiative heat transfer coefficient K_r is a sum of vial-bottom and vial-top emissivity (e_s and e_v), as expressed by following approximated equation (Pikal et al., 1984, the coefficient of Eq. (13) in the literature):

$$K_r = 4\sigma \bar{T}^3 (e_s + e_v) \quad (4)$$

where $\bar{T}$ is the average temperature. The condition of using this approximation, as indicated by Pikal et al. (1984, page 1226) is "for temperature normally used in freeze-drying". In order to use the approximation $4\sigma\bar{T}^3 = 1.0 \times 10^{-4}$, the average value of the shelf temperature T_s and the product temperature T_b, denoted as $\bar{T}$, should be approximately 264.5 K (−47 °C). In addition, it is necessary to assume $T_i \approx T_s$ in Eq. (1) to omit the last term of the equation. Strictly speaking, in order to use the simplified Eqs. (2) and (3) properly, it may be necessary to assign different values for $4\sigma\bar{T}^3$ for different ranges of the average temperature if $\bar{T}$ is significantly deviated from −4.7 °C. The value of $4\sigma\bar{T}^3$ appears to be a linear function of the average temperature $\bar{T}$. Thus its appropriate value for a corresponding value of the average temperature can be computed automatically for self-developed computer source codes such as FORTRAN using this linear equation. A commercially available software package may not have this flexibility.

The conductive heat transfer coefficient of the gas between the shelf and glass vial K_g is expressed by:

$$K_g = \frac{\alpha \Lambda_0 P_c}{1 + \ell_v(\alpha \Lambda_0 / \lambda_0) P_c} \quad (5)$$

where P_c is the chamber pressure, Λ_0, the free molecular heat conductivity of the gas at 0 °C, equal to 6.34×10^{-3} cal s^{-1} °C^{-1} cm^{-2} mmHg^{-1}; λ_0, the thermal conductivity of gas at ambient temperature, equal to 4.29×10^{-5} cal s^{-1} °C^{-1} cm^{-1}, and α is defined by

$$\alpha = \frac{a_c}{2 - a_c} \left(\frac{273.2}{T} \right)^{1/2} \quad (6)$$

In Eq. (4), a_c is the energy accommodation coefficient. The value of α is approximately equal to 0.52. From Eqs. (3) and (5), it can be seen that K_v is a function of the chamber pressure.

Since the approach used in this paper, for solving the heat and mass transfer equations, does not require using the simplified equation Eq. (2), Eq. (1) will be used instead. The purpose of using Eq. (1) is to perform the computations as accurate as possible, although the computational error of using Eq. (2) on the resulting product temperature T_b may not be very significant. With the pseudo-steady state assumption described earlier, the temperature profile, across the frozen layer at any drying time, can be regarded as linear. The rate of heat conduction through the frozen product becomes:

$$Q = -A_v \cdot K_I \frac{dT}{dX} = -A_v \cdot K_I \frac{T_i - T_b}{\ell_m - \ell} \quad (7)$$

where K_I is the effective thermal conductivity of the frozen layer, T_i the temperature at the receding surface of the frozen layer, ℓ_m the maximum thickness of the frozen layer, and ℓ is the thickness of the dry layer which is a function of time. Thus $\ell_m - \ell$ becomes the thickness of the frozen layer during primary drying. The following conversion factor between the heat and mass transfer rates was obtained from the literature (Pikal et al., 1984):

$$Q\,(\text{cal/s}) = 0.1833 \frac{dm}{dt} \quad (8)$$

where dm/dt is the sublimation rate in g/h, and the coefficient 0.1833 is the factor to convert the sublimation rate of pure water from g/h to cal s^{-1}.

2.2. Solution of heat and mass transfer equations

The heat and mass transfer equations used in this paper are not identical to those in the literature (Pikal, 1985, Eqs. (34)–(39) in the literature). For example, Eq. (1) was used to describe the vial heat transfer rate, rather than the simplified Eq. (2). Furthermore, the algorithms used in this paper for solving these equations (as indicated by Eqs. (22)–(24)) and to perform the simulation are different from that used in the literature. Therefore, it is necessary to clearly list these equations here. For convenience of subsequent derivations, the following new variables are introduced in this paper:

$$Y_1 = \frac{\mathrm{d}m}{\mathrm{d}t} \tag{9}$$

$$Y_2 = T_\mathrm{s} \tag{10}$$

$$Y_3 = T_\mathrm{t} \tag{11}$$

$$Y_4 = T_\mathrm{b} \tag{12}$$

$$Y_5 = T_\mathrm{i} \tag{13}$$

and

$$Y_6 = P_\mathrm{v} \tag{14}$$

with the substitutions of Eqs. (1) and (7)–(14), the heat and mass transfer equations can be written as

$$F_1 = Y_1 - \frac{\mathrm{ASV}\cdot K_\mathrm{s}}{0.1833}(T_\mathrm{f} - Y_2) = 0 \tag{15}$$

$$F_2 = Y_1 - \frac{ATV\cdot K_\mathrm{tr}}{0.1833}(Y_2 - Y_3) = 0 \tag{16}$$

$$F_3 = Y_1 - \frac{A_\mathrm{v}(K_\mathrm{c}+K_\mathrm{g})}{0.1833}(Y_3 - Y_4) - \frac{A_\mathrm{v}e_\mathrm{s}\sigma}{0.1833}(Y_3^4 - Y_4^4) - \frac{A_\mathrm{v}e_\mathrm{v}\sigma}{0.1833}(Y_2^4 - Y_5^4) = 0 \tag{17}$$

$$F_4 = Y_1 + \frac{A_\mathrm{v}K_\mathrm{I}}{0.1833}\frac{Y_5 - Y_4}{\ell_\mathrm{m} - \ell} = 0 \tag{18}$$

$$F_5 = Y_1 - \frac{1}{R_\mathrm{s}+R_\mathrm{p}}(P_0 - P_\mathrm{c}) = 0 \tag{19}$$

$$F_6 = Y_1 - (Y_6 - P_\mathrm{c})\left[S_0 + \frac{S_1}{2}(Y_6 + P_\mathrm{c})\right] = 0 \tag{20}$$

In Eq. (19), R_p is the dry layer resistance, defined as the normalized dry layer resistance R_pN divided by the cross-sectional area of the product, as

$$R_\mathrm{p} = \frac{R_\mathrm{pN}}{A_\mathrm{p}} \tag{21}$$

and R_pN is expressed in terms of the three parameters (product resistance parameters) R_0, A_1, and A_2:

$$R_\mathrm{pN} = R_0 + \frac{A_1\ell\ell}{1 + A_2\ell\ell} \tag{22}$$

In Eq. (19), P_0 is the equilibrium chamber pressure in mmHg, which can be expressed by

$$P_0 = 2.6983\times 10^{10}\exp\left(\frac{-6144.96}{Y_5}\right) \tag{23}$$

Eqs. (15)–(20) become simultaneous nonlinear algebraic equations for the six variables, Y_1–Y_6. These equations can be solved by the Newton–Ralphson iteration method (Carnahan et al., 1969). Given initial estimates of Y_i (i = 1–6). Eqs. (13)–(18) can be linearized using Taylor series expansion in a neighborhood of Y_i^*, by truncating higher order terms, as given below:

$$\left(\frac{\partial F_i}{\partial Y_1}\right)^*(Y_1 - Y_1{}^*) + \left(\frac{\partial F_i}{\partial Y_2}\right)^*(Y_2 - Y_2^*) + \left(\frac{\partial F_i}{\partial Y_3}\right)^*(Y_3 - Y_3^*) + \left(\frac{\partial Fi}{\partial Y4}\right)^*(Y4 - Y4^*) + \left(\frac{\partial F_i}{\partial Y_5}\right)^*(Y_5 - Y_5^*) + \left(\frac{\partial F_i}{\partial Y_6}\right)^*(Y_6 - Y_6^*) = -F_i^*,$$

$$i = 1\text{–}6 \tag{24}$$

where Y_1^*–Y_6^* are the initial estimates of Y_1–Y_6, respectively. F_i^* denotes the values of F_i (i = 1–6) evaluated using the estimates of Y_i^*. $(\partial F_i/\partial Y_j)^*$ represents the derivatives of F_i versus Y_j (j = 1–6), evaluated using the starting values (initial estimates) Y_i^*. This is also termed the Jacobian matrix $\mathbf{J}$, and each element of J_{ij}, can be expressed by

$$J_{ij} = \frac{\partial \mathbf{F}_i}{\partial \mathbf{Y}_j} \tag{25}$$

where the bold-faced $\mathbf{F}$ and $\mathbf{Y}$ denote the vector and tensor forms. The elements of the Jacobian matrix, $\partial\mathbf{F}_i/\partial\mathbf{Y}_j$, for the six simultaneous nonlinear algebraic equations are obtained from Eqs. (15)–(21).Eq. (24) represents six simultaneous algebraic equations which car; be solved for Y_i using Gauss elimination method (Carnahan et al., 1969). Improved estimates for Y_i can then be obtained from the following equation:

$$\mathbf{Y}^{k+1} = \mathbf{Y}^k - [\mathbf{J}^k]^{-1}\cdot\mathbf{F}^k, \quad k = 1\text{–}6 \tag{26}$$

where k denotes the kth iteration, and $\mathbf{J}$ is the Jacobian matrix in vector form, and $[\mathbf{J}^k]^{-1}$ is the inverse of the matrix. The final results are regarded as successfully achieved when there is no further improvement in $\mathbf{Y}^{k+1}$.

2.3. Ramping of shelf temperature

The cycle runs for 5% mannitol and the seven formulations in Table 1 were performed using shelf temperature ramping, rather than "jumped" directly, from the freezing temperature to the primary drying shelf temperature. For 5% mannitol, the ramping was 0.42 °C/min from −40 to −15 °C with a duration of 60 min. For the seven formulations in Table 1, the ramping was 0.44 °C/min from −40 to −20 °C with a duration of 45 min. The sublimation of ice during ramping depends on the ramping rate and may not be negligible. Therefore, in the primary drying subroutine PDRYS, the shelf fluid temperature needs to be varied

Table 1
Formulations studied in this paper

Formulation no.	Formulation
1	Sucrose: 3.42 mg/mL; glycine: 3.75 mg/mL; NaCl: 0.58 mg/mL; LDH: 50 mg/mL; (pH 5.99)
2	Lactose: 30 mg/mL; sucrose: 3.42 mg/mL; glycine: 3.75 mg/mL; NaCl: 0.58 mg/mL; LDH: 50 mcg/mL; (pH 5.85)
3	Mannitol: 30 mg/mL; sucrose: 3.42 mg/mL; glycine: 3.75 mg/mL; NaCl: 0.58 mg/mL; LDH: 50 mcg/mL; (pH 5.96)
4	Sucrose: 33.42 mg/mL; glycine: 3.75 mg/mL; NaCl: 0.58 mg/mL; LDH: 50 mcg/mL; (pH 5.96)
5	Lactose: 30 mg/mL; LDH: 50 mcg/mL; (pH 5.46)
6	Mannitol: 30 mg/mL; LDH: 50 mcg/mL; (pH 5.68)
7	Sucrose: 30 mg/mL; LDH: 50 mcg/mL; (pH 5.60)

over time, rather than using a fixed value. This was performed using the following FORTRAN statements:

```
IF (TIME.LT. T_RAMP) THEN
    TF = TF0 + TF_RATE*DELT
ELSE
    TF = TF1
ENDIF
```

where TIME, is the run time, T_RAMP the ramping time, TF the instantaneous shelf fluid temperature, TF0 the initial shelf fluid temperature at the onset of ramping, TF_RATE the ramping rate, DELT the time interval of the integration, and TF1 is the primary drying shelf temperature after ramping. The shelf temperature is the most important factor affecting the product temperature. In order to ensure the accuracy of computation during ramping, DELT was set at 1 min. It is clear that during the simulation process, the shelf temperature varies over time, but was not treated as a dependent variable. It was controlled directly by the software of the freeze dryer. Since the FORTRAN source code for the primary drying subroutine was self-developed, it can be easily modified to accommodate the shelf ramping effect.

2.4. Computation procedures of primary drying process

The entire computation scheme is illustrated by the flow diagram in Fig. 1. The following given constants are necessary to perform the computations: (1) the shelf and chamber constants: KTC, KTP, KTD, KP, KD, T_f and P_c; (2) the vial and formulation constants: ATV, A_v, A_p, K_I, and ℓ_m; (3) the product resistance parameters: R_0, A_1, and A_2. The values of other coefficients and constants, such as K_g, KD, R_s, and K_{tr}, are then computed. The time interval Δt, denoted as DELT in the FORTRAN program, is chosen. The typical value of Δt used is from 1 to 10 min. The solution for the dependent variables in the six simultaneous algebraic equations was performed by the Newton–Ralphson iteration algorithm, as indicated by Eqs. (15)–(20), started from time zero. With the initial estimates Y_i^*, the values of the F_i^* (Eqs. (15)–(20)) and J_{ij}^* (Eq. (23)) are evaluated. These values are then substituted into Eq. (22). The resulting six linear algebraic equations are then solved using the Gauss elimination technique (Carnahan et al., 1969). If the convergence criteria are not satisfied, the new values of Y_i are substituted for Y_i^* in Eq. (24), and the iteration procedure is repeated until successful

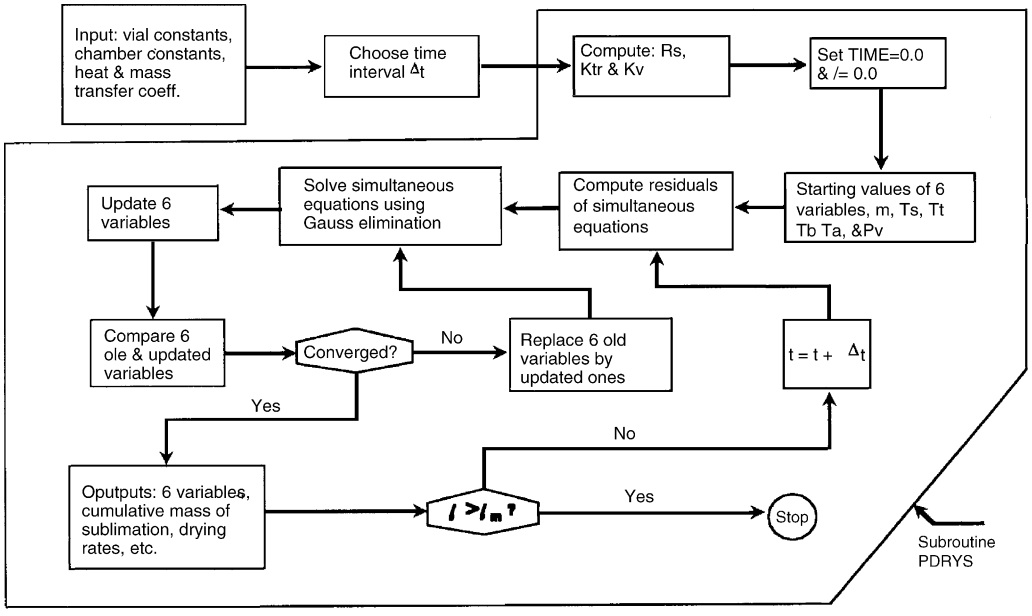

Fig. 1. Computation scheme for the primary drying subroutine PDRYS.

convergence is reached. The final results are regarded as successfully achieved when there is no further improvement in Y_i. The computed results at each time point include the six dependent variables dm/dt, T_s, T_t, T_b, T_i and P_v, as well as M_t and ℓ. This completes the first computational step.

The next computational step is to update the dry layer thickness ℓ. The accumulated mass of sublimation for either option is also computed as follows. The change in the sublimed mass ΔM_t in each computational step is first computed by

$$\Delta M_t = (\text{Rate})_{\text{avg}} \cdot \frac{\Delta t}{60} \tag{27}$$

where $(\text{Rate})_{\text{avg}}$ is the average rate of sublimation in g/h, between two computational steps. The change in the frozen layer thickness ℓ is then obtained as

$$\Delta \ell = \frac{4 \cdot \Delta M_t}{\pi d^2 \rho} \tag{28}$$

where ρ is the density of the frozen layer, which is approximately equal to 0.917. $(1 - y)$ where y is the fraction of total solid (Pikal, 1985); d the inside diameter of the vial. Thus the accumulated dry layer thickness ℓ and sublimation mass M_t become:

$$\ell = \ell + \Delta \ell \tag{29}$$

and

$$M_t = \sum (\text{Rate})_{\text{avg}} \cdot \frac{\Delta t}{60} \tag{30}$$

with the FORTRAN source codes developed, the following dependent variables versus time profiles during the entire primary drying period can be readily computed: dm/dt, T_s, T_t, T_b, T_i, P_v, M_t and ℓ.

2.5. Powell's optimization algorithm—to search for the product resistance parameters

The computation scheme for the nonlinear parameter estimation is depicted in Fig. 2. It comprises two computation (or iteration) loops. The inner loop, as shown in Fig. 1, is the Newton–Ralphson iteration for solving the simultaneous heat and mass transfer equations, Eqs. (15)–(20). The outer loop is Powell's nonlinear parameter estimation algorithm in Fig. 2, where the best-fit values of the parameters are obtained by minimizing the following sum of the squares, SSQ:

$$\text{minimize(SSQ)} = \text{minimize}\left(\sum_{i=1}^{n}[(T_b(t) - T_{bi})]^2\right) \tag{31}$$

where n is the number of data points; $T_b(t)$ and T_{bi} are the theoretically and experimentally determined product temperatures, respectively. The first sets of input data include: (1) vial constants, (2) chamber constants, (3) time increment for pseudo-steady state integration t, (4) initial estimates of the product resistance parameters defined in Eq. (22). The experimental input data are the product temperature profiles of T_b, and the parameters to be determined are the dried layer product resistance parameters R_0, A_1 and A_2. For each data point of T_{bi}, the program searches through the primary drying subroutine PDRYS for the theoretical value of $T_b(t)$ at the run time equal to the sampling time for the data point. The above computation was repeated until all data points are computed. After the theoretical values of $T_b(t)$ are obtained, Eq. (31) is then used to compute the sum-of-squares SSQ. For each iteration, if the discrepancy is high between the experimental and computed data, the values of the initial estimates of the parameters are adjusted until no further improvement is observed. This adjustment procedure is Powell's algorithm to minimize the SSQ in Eq. (31). The result-

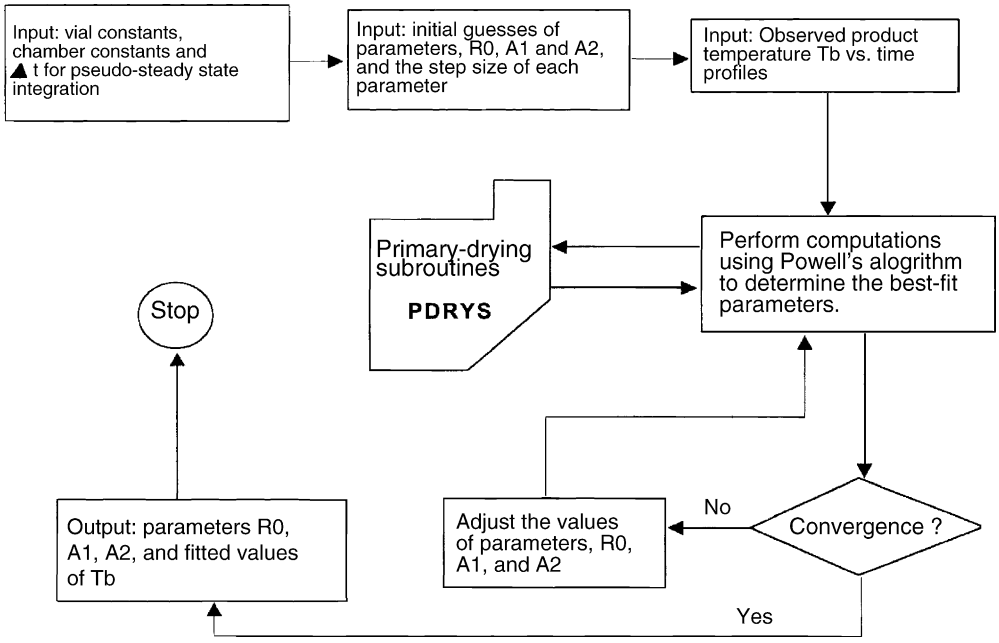

Fig. 2. Computation scheme of Powell's sum-of-squares minimization algorithm in conjunction with the primary drying subroutine.

ing values of the parameters are the final solutions for the dried layer product resistance parameters. The preceding procedure is equivalent to the nonlinear least squares algorithm. Due to the versatility of Powell's algorithm, the parameters can be determined as the "best-fit" values over the entire time course of the primary drying.

2.6. Comparison of the proposed approach with the nonlinear regression approach in the literature

The mathematical approach for determination of the mass transfer parameters using measured product temperature profiles is somewhat similar to the regression analysis to determine the regression parameters P_i, $K'T_v/R_{pN}$ and K_v description by Milton et al. (1997, page 9), except the three aspects described later. The Powell's algorithm used in this paper is similar to the Marquardt–Levenberg algorithm used by Milton et al. Both algorithms use an iterative process to adjust the model parameters until the profile of the chosen dependent variable "fits" the experimental data. The program continues to adjust the parameters until the residual sum of squares has been minimized.

The three different aspects are: (1) the dependent variable in this paper is the product temperature T_b, instead of the chamber pressure by Milton et al.; (2) the parameters in this paper are the dry layer mass transfer parameters, while the parameters by Milton et al. are P_i, $K'T_v/R_p$ and K_v; (3) Eq. (1) of Milton was replaced by the entire primary drying subroutine PDRYS depicted in Fig. 1, and this is the major difference from Milton, as described below.

The product temperature T_b cannot be derived and expressed as a simple equation such as Eq. (1) of Milton. This is due to the complex heat and mass transfer mechanisms surrounding the product vial. It can only be obtained numerically by solving Eqs. (9)–(26) for each time point. After solving these equations numerically, the product temperature T_b can be obtained for the entire primary drying, at any selected time points, with a given set of the mass transfer parameters R_0, A_1 and A_2. Now, the next step is to link PDRYS to Powell's nonlinear regression algorithm. This is performed by modifying the FORTRAN source code of Powell's algorithm which is available in the literature (Kuester and Mize, 1973; Kuu et al., 1992). One of the important features of Powell's algorithm is that that it does not require "explicit equations" to perform regression. It only requires the "computed numerical values" of the product temperature at various time points. This is the reason why the complex computation subroutine PDRYS can be easily linked to Powell's main program.

The procedure of PDRYS to compute the product temperature at selective time points is described below. First, during the cycle run, the product temperature profile for each formulation was measured and recorded for the entire primary drying. For the case of the LyoStar™ II dryer used in this work, the product temperature can be recorded every minute. The next step is to choose appropriate time intervals from the obtained product temperature profile for regression analysis. It is not necessary and impractical to use all the data points for the computations, since the number of data points could be several thousands for the recording time of every minute. Normally it is sufficient to use 20–50 data points, to describe the entire primary drying. For the purpose of explanation, the selected experimental time and temperature are denoted as Time(i) and T_{bi}, respectively, where $i = 1$–N, and N is the number of the data points. During the regression process, for each set of input mass transfer parameters R_0 A_1 and A_2, the program in Fig. 2 computes the product temperature T_b started from time zero. To keep tracking of the progress of primary drying, the program continues to compute the product temperature with the selected time increment t, where t was chosen as 1 min in this paper. In this way, the entire T_b profile was obtained. In the mean time, during the computation process, the program was designed to automatically "pick" the computed product temperature T_b when its corresponding time point matches the experimental time point Time(i). The resulting temperature profile is equal to $T_b(t)$ in Eq. (31).

2.7. Comparison of the approach used in this paper with that used by Kuu et al. (1995)

The approach used in the paper by Kuu et al. (1995) was based on the heat and mass transfer equations for primary drying developed by Pikal et al. (1984) and Pikal (1985). The source codes were developed for two options: (1) using the sublimation data as the input data for the dependent variable at selected time points, and (2) using product temperature as the input data, at selected time points, for the dependent variable. The methodology used in this paper is an expansion of the paper by Kuu et al. The expansion includes the following: (1) the nonlinear parameter estimation was performed using the "entire product temperature profile" rather than selected time points; (2) the FORTRAN source codes were updated to include shelf temperature ramping effect; (3) a robust method for estimation of the initial estimate of the parameters was added. Without this feature, it is very difficult to obtain an appropriate initial estimates of the parameters; (4) the vial heat transfer rate Eq. (1) was used, rather than the simplified equation $Q = A_v K_v (T_f - T_b)$ to improve the accuracy of computing the heat transfer rate around the vial.

2.8. A robust shortcut for searching initial estimates of parameters

In order to obtain the final solutions for the product resistance parameters, it is critical to start with appropriate values of initial estimates for these parameters. The requirement of initial estimates is the nature of solving simultaneous nonlinear equations. A commonly used method is by trial-and-error, by arbitrarily choosing combinations of these parameters and testing the convergence of computations. But this method becomes very difficult when the number of parameters is >2. A robust short-cut approach, including the following steps, can be used to quickly determine the appropriate initial estimates:

(1) Determine the range of each parameter.
(2) Divide the range of each parameter into a number of divisions. For example, if each of the three parameters R_0, A_1 and

A_2 is divided into 10 divisions, there are 1331($11 \times 11 \times 11$) combinations to be tested.
(3) Set-up a table for all combinations of the parameters.
(4) Compute SSQ (the sum of squares) for each combination of parameters using the primary drying subroutine PDRYS.
(5) Sort the resulting values of SSQ in an ascending order.
(6) Perform Powell's parameter estimation process starting from the parameters with the smallest value of SSQ.

With an appropriate design of the FORTRAN source codes, the computations for steps 1–6 can be performed automatically. Numerical experiences indicate that the optimum parameters of R_0, A_1 and A_2 can be rapidly determined using the obtained values of initial estimates described in the above procedure.

3. Materials and methods

As described in Section 1, the heat transfer parameters, K_s, e_v, e_s, K_{cs}, and ℓ_v are specific to the dyer and vial used, and have been determined by Pikal (1985) and Pikal et al. (1984, 1983) for several types of dryer and vials. If these parameters are not available, they can be determined using the following relatively simple experiments. As indicated earlier, these parameters are only required to be determined once, assuming that the same types of dryer and vial are used for all freeze-drying studies. Since freeze-drying of pharmaceutical product is generally performed in production settings that do not use trays in the dryers, the following experiments were performed without a tray.

3.1. Determination of radiation emissivities and shelf heat transfer coefficients

The values of the shelf surface emissivity for both the LyoStar™ and Edwards dryers were measured using the Omega OS205 Infrared Pyrometer (Omega Engineering Inc., Omega.com). the shelf surface emissivity is constant for a particular dryer at a particular point in time, independent of the formulation or vial type used. For measurements, thermocouples were placed at various locations of the shelf surface, so that actual temperatures of the shelf surface could be measured. The sensor of the pyrometer was then aimed at the location of shelf surface adjacent to each thermocouple. The emissivity of the pyrometer was adjusted until the temperature reading on the pyrometer was the same as the temperature measured by the thermocouple at the particular location.

For determination of the vial-top radiation emissivity e_v, Pikal (1985) proposed an approach for measuring the top emissivity e_v. In this paper, e_v was generated by using the single vial procedure and adjusting the shelf temperature so that the shelf surface temperature T_s is equal to the product temperature at the bottom of the vial T_b. Under these conditions, the heat transfer was due to the top radiation term only. This approach appears to be very logical. The resulting e_v was determined to be approximately 0.84 and independent of the types and sizes of vials tested. Since the experiment requires a highly modified laboratory dryer, it was very difficult (or impossible) to be performed in the dryers available to us. Therefore, this value was used for the simulation studies in this paper. As with the surface emissivity, the vial-top emissivity is independent of formulation or type of vial, depending only on the dryer to be used.

The approach used in this paper for determination of the shelf heat transfer coefficient K_s is based on two conditions: (1) lyophilizing the product in vials with previously determined heat transfer coefficient K_v, and (2) the product temperature T_b and shelf internal temperature T_f profiles are recorded during the entire course of primary drying. In this way, the temperature difference ($T_f - T_b$) at each time point can be determined. This approach is similar to that used by Pikal et al. (2005) for determination of the vial heat transfer coefficient K_v. The detailed calculations for the shelf heat transfer coefficient are described in Appendix A.

3.2. Determination of vial heat transfer parameters K_{cs} and ℓ_v using weight loss data of frozen pure water

The weight loss experiment was performed using a LyoStar™ freeze-dryer. A full shelf of washed and depyrogenated 10 mL/20 mm vials (Schott Pharmaceutical Inc.) were filled with 6.7 mL of 0.22 μm filtered Milli-Q water and partially stoppered with sterile stoppers. Selected vials were weighed and loaded into the dryer. The following cycle was run: (1) ramp from 20 to −25 °C in 30 min (1.8°/min); (2) dwell at −25 °C for 4 h; (3) turn on vacuum and wait until 100 μm is reached; (4) ramp to 10 °C in 30 min (1.2°/min); (5) dwell at 10 °C, 100 μm, for 8 h. After completion of the cycle run, the vials were stoppered and allowed to return to ambient temperature, and the selected vials were again weighed. The amount of water lost during sublimation was calculated. Approximately 59–63% of the water in the vial was sublimated at the end of experiment.

The product resistance for frozen pure water has been presented by (Pikal et al., 1983, Table 1). It reflects the resistance in transforming water from the solid state to the vapor state (i.e. the phase change) plus the resistance in transport of water vapor from the ice–vapor interface to the top of the capillary tube used in the microbalance experiment. The results in Pikal's Table 1 indicate that the resistance appears to be pressure-dependent. Based on the values of R_0 and A_1 at the chamber pressure of 0, 0.176 and 0.309 Torr, the values of R_{pN} were calculated at the dry layer thickness of 0–1.0 cm. At each data point, interpolation was performed for each data point to determine the R_{pN} at 0.1 Torr. The resulting values of R_{pN} at 0.1 Torr were then analyzed using linear regression. The resulting product resistance equation for the pure frozen water becomes $R_{pN} = 0.0993 + 0.1889\ell$.

The resistance of the stopper vent R_s can be expressed by $R_s = 1/(S_0 + S_1 P_{av})$, where S_0 and S_1 are constants and P_{av} is the average pressure of the vial P_v and chamber P_c (Pikal, 1985). The effect of the variability of the resistance of the vial stopper vent on the sublimation rate, due to the variation of stopper placement, can be simulated using the primary drying subroutine PDRYS. For example, the following input parameters for PDRYS are: $A_v = 4.43$, $A_p = 3.58$, $V = 6.7$ mL, $R_0 = 0.0993$, $A_1 = 0.1889$, PC = 0.1 Torr, $T_f = 273$ K, fill volume = 5 mL. Other parameters (KTC, KTP, KTD, KC, KD, KP, K_I, K_s, K_{cs}, ℓ_v,

Table 2
Effect of stopper resistance parameters S_0 and S_1 on the amounts of water removed by sublimation at various drying time

Drying time (h)	Amount of water removed (g)		
	$R_s = 0.0435$[a] ($S_0 = 4.8$, $S_1 = 169$)	$R_s = 0.0833$[a] ($S_0 = 2.4$, $S_1 = 84$)	$R_s = 0.0224$[a] ($S_0 = 9.2$, $S_1 = 340$)
4	1.422	1.390	1.441
8	2.864	2.791	2.891
10	3.576	3.497	3.622
12	4.302	4.208	4.357

[a] The value of the stopper resistance R_s is in (cm^2 Torr h g^{-1}).

e_s, e_v, σ, and λ_0) are the same as those in Fig. 4. The stopper resistance parameters for a 20 mm neck vial are $S_0 = 4.8$ and $S_1 = 169$ (Pikal, 1985). To study the effect of stopper resistance on the sublimation rate, the stopper resistance parameters S_0 and S_1 were varied for each simulation run using PDRYS. The resulting simulated amounts of water removed by sublimation at various values of the stopper resistance R_s, calculated by the equation $R_s = 1/(S_0 + S_1 P_{av})$, are summarized in Table 2. It is clear that the effect: of the variation of the stopper resistance, due to the variation of stopper placement, on the rate of sublimation is negligible.

The vial-bottom heat transfer parameters K_{cs} and ℓ_v are independent of formulation, depending only on the vial and the dryer to be used. In order to separate the effect of the pressure and temperature ramping up period from the actual sublimation phase, a separate run was performed from time zero to the time when the target shelf temperature and chamber pressure was reached. The resulting amount of sublimation is used as the baseline to be excluded from the actual primary drying runs. After obtaining the weight loss data and the product resistance equation for the pure frozen water described above $R_{pN} = 0.0993 + 0.1889\ell$, Powell's nonlinear parameter estimation algorithm was then used to obtain K_{cs} and ℓ_v. The results are discussed in Section 4.2.

3.3. Freeze-drying cycle runs for various formulations to obtain the product temperature profiles T_b during primary drying

After obtaining the heat transfer parameters, K_s, e_v, e_s, K_{cs}, and ℓ_v, the final experiment is to perform a cycle run for the formulation of interest. For 5% mannitol, 3 mL of the the formulation was filled into both Schott and Wheaton 10 mL tubing vials and placed on the same shelf. The stopper used was the two-leg 20 mm lyophilization stopper (Wheaton gray butyl stopper, part number 22410-194). For each vial type, five center vials were probed with 30 gauge thermocouples (FTS Systems Inc., part number FDPS20) at the bottom-center of the vial. In this way the product temperature profiles of these two types of vials can be directly compared. The cycle parameters are: (1) precool shelves to 5 °C; (2) freeze shelves to −40 °C (0.5 °C/min); (3) hold at −40 °C for 2 h; (4) adjust chamber pressure to 100 mT; (5) increase shelf temperature to −15 °C (0.4 °C/min); (6) maintain shelf temperature of −15 °C for 40 h; (7) increase shelf temperature to +45 °C (1.3 °C/min); (8) maintain at +45 °C for 2 h; (9) neutralize chamber, stopper vials.

The formulations, containing lactose dehydrogenase (LDH), studied in this paper are listed in Table 1. Thermocouples were placed at the bottom-center of the center vials in order to measure the maximum product temperature within the vial T_b. For freeze-drying of these formulations, the dryer, vial and cycle parameters are listed below. Freeze-dryer: LyoStar™, FTS Systems; vial: Schott 10 mL tubing vial. The following cycle was run: (1) cooling: 5 h ramp to −40 °C; (2) freezing: 2 h dwell at −40 °C; (3) primary drying: start vacuum, set to 100 μm, 45 min ramp from −40 to −20 °C; (4) primary drying: 15 h dwell at −20 °C; (5) secondary drying: 35 min ramp from −20 to +40 °C; (6) secondary drying: 4 h dwell at +40 °C.

4. Results and discussion

4.1. Radiation emissivities and shelf heat transfer coefficients

The measured shelf surface emissivity using an Omega® infrared pyrometer for both the LyoStar™ and Edwards dryers is approximately 0.6. This value is very close to the values reported in the literature for polished 316 stainless steel (Pikal et al., 1984). The shelf heat transfer coefficient K_s of the LyoStar™ dryer was determined using the product temperature profile of 5% mannitol in 10 mL Wheaton tubing vials, in the interior (center) location of the shelf, as presented in Fig. 4. Since the two heat transfer parameters of the Wheaton vial have be determined by Pikal et al. (1984), the vial heat transfer coefficient K_v at various levels of the chamber pressure and shelf temperature can be calculated. As such, K_s can be determined using the similar approach as that used by Pikal et al. (2005) for determination of the vial heat transfer coefficient. The detailed procedure is presented in Appendix A. The obtained value of K_s for the LyoStar™ II dryer is equal to 0.0024 cal s^{-1} cm^{-2} °C^{-1}.

4.2. Vial heat transfer parameters: contact parameter K_{cs} and separation distance ℓ_v

After obtaining the weight loss data from the sublimation of frozen pure water, during primary drying, the vial heat transfer parameters K_{cs} (the contact parameter) and the separation distance ℓ_v, can be determined by the following computation procedure. Computations for these two parameters were performed using Powell's nonlinear parameter estimation algorithm presented in Fig. 2. This is similar to Section 4.3 with the following conditions: (1) the dependent variable is the

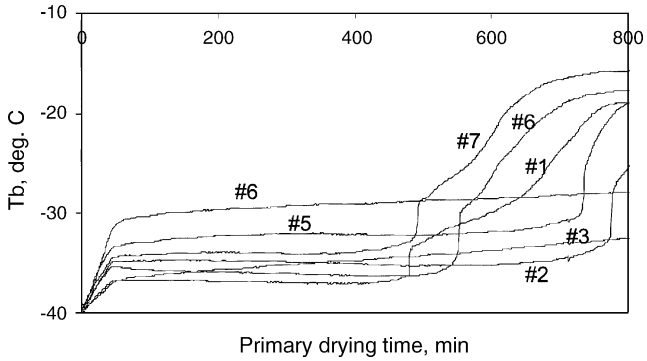

Fig. 3. Product temperature profiles of various formulations during primary drying.

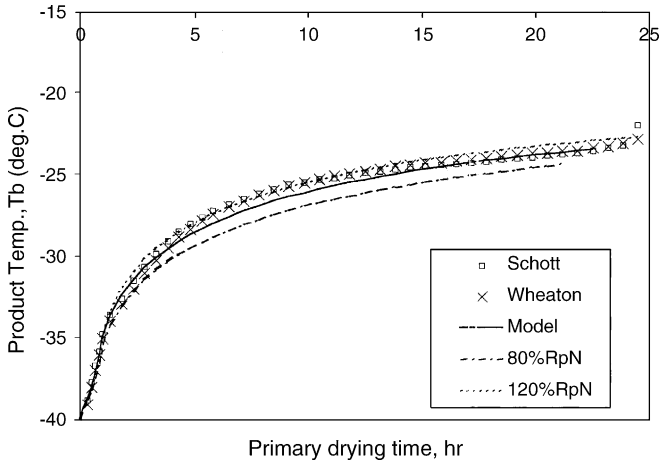

Fig. 4. The experimental and simulated product temperature vs. time profiles of 5% mannitol in 10 mL tubing vial during primary drying as a function of the shelf fluid temperature, $R_{pN} = 2.025 \times 10^{-4} + 20.23\ell$. Constants and parameters used for the simulation are listed below (detailed explanations for other symbols can be found in the literature (Pikal, 1985), also in Nomenclature of this paper). Large values of KTC and KTP were chosen to simulate the primary drying without using trays: $A_v = 4.43$, $A_P = 3.58$, $R_0 = 0.0002025$, $A_1 = 20.23$, KTC = 100.0, KTP = 100.0, KTD = 1.0, KC = 2.64×10^{-4}, KD = 3.64, KP = 3.32×10^{-3}, $K_I = 0.0059$, $K_s = 0.0024$, $S_0 = 4.8$, $S_1 = 169.0$, $K_{cs} = 1.19 \times 10^{-4}$, $\ell_v = 0.0551$, $e_s = 0.60$, $e_v = 0.84$, $\sigma = 1.35 \times 10^{-12}$, $\lambda_0 = 4.29 \times 10^{-5}$. The parameters KTC, KTP, KIT, KC, KD, KP, K_I, S_0, and S_1 were determined by Pikal et al. (1984) and Pikal (1985); K_{cs} and ℓ_v for the Schott 10 mL tubing vial were determined in this work. Units of the parameters and constants can be found in the Nomenclature.

amount of water sublimated during primary drying; (2) the product resistance equation for frozen pure water is $R_{pN} = 0.0993 + 0.1889\ell$; (3) the stopper resistance is negligible, as described in Section 3.2. The obtained values for the Schott 10 mL tubing vial are: $K_{cs} = 1.19 \times 10^{-4}$ cal s^{-1} cm^{-2} °C^{-1}, $\ell_v = 0.0551$ cm. By comparison, the values of K_{cs} and ℓ_v for 10 mL Wheaton tubing vial obtained by Pikal et al. (1984) are 1.24×10^{-4} cal s^{-1} cm^{-2} °C^{-1} and 0.0471 cm, respectively. After obtaining K_{cs} and ℓ_v, the vial heat transfer coefficient K_v can be calculated using Eqs. (3)–(6). The resulting values of K_v for Schott and Wheaton 10 mL tubing vials, at the chamber pressure 100 mTorr (0.1 Torr), are 4.98×10^{-4} and 5.13×10^{-4} cal s^{-1} cm^{-2} °C^{-1}, respectively. Therefore, the difference in K_v for these two types of vial is negligible. This can also be confirmed by the primary drying of 5% mannitol in Fig. 4, where both Schott and Wheaton 10 mL tubing vials were placed on the same shelf, in the center area of the shelf. The resulting two product temperature profiles, average of five vials for each vial type, are nearly identical.

4.3. Product temperature T_b and product resistance parameters of various formulations

The normalized dried layer mass transfer resistance of various formulations is expressed by Eq. (20). The product resistance parameters R_0, A_1 and A_2 were determined using the T_b profile in Figs. 3 and 4 and Powell's nonlinear parameter estimation algorithm in Fig. 2. The resulting parameters for eight formulations are presented in Table 3. The experimental product temperature and the theoretical product temperature profiles, simulated using these parameters, are presented in Figs. 4–8. It can be seen the close agreement between these two profiles, indicating the suitability of the proposed approach for determination of the product resistance parameters. For the formulations containing mannitol, Figs. 4, 5 and 8, the T_b values increase with the drying time until the completion of primary drying, indicating the increase of product resistance. For this type of T_b profile, both the maximum T_b and primary drying time can be closely simulated.

Table 3
Resulting mass transfer resistance parameters R_0, A_1 and A_2 obtained from the parameter estimation approach

Formulation #	R_0	A_1	A_2
5% Mannitol (3 mL)	0.0002025	20.23	0
1	0.2966	13.56	223.0
2	1.067	31.54	166.7
3	0.3861	2.490	−0.6764
4	1.102	−11.80	25.59
5	1.771	23.46	11.62
6	4.277	17.29	0.0
7	1.443	1.901	0.0

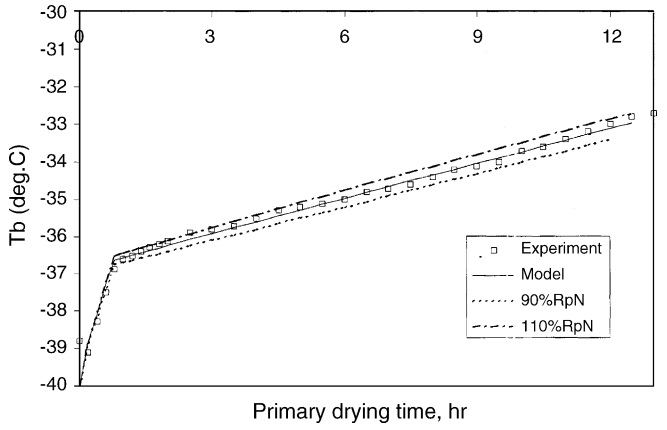

Fig. 5. The experimental and simulated product temperature vs. time profiles for Formulation #3, $R_{pN} = 0.3861 + 2.490\ell/(1 - 0.6764\ell)$. The constants and parameters used for the simulation are the same as those of Fig. 4, except R_0, A_1 and A_2.

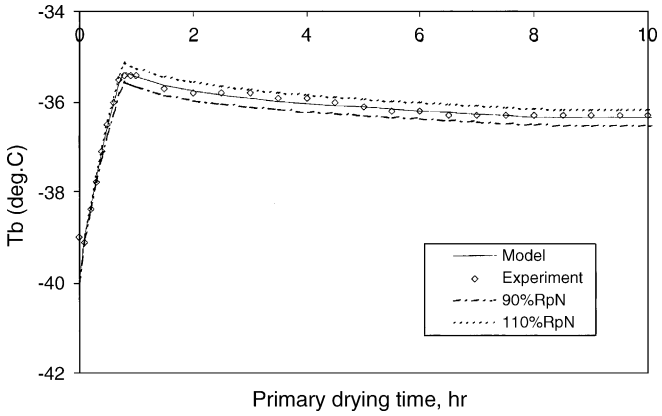

Fig. 6. The experimental and simulated product temperature vs. time profiles for Formulation #4, $R_{pN} = 1.102 - 11.80\ell/(1 + 25.59\ell)$. The constants and parameters used for the simulation are the same as those of Fig. 4, except R_0, A_1 and A_2.

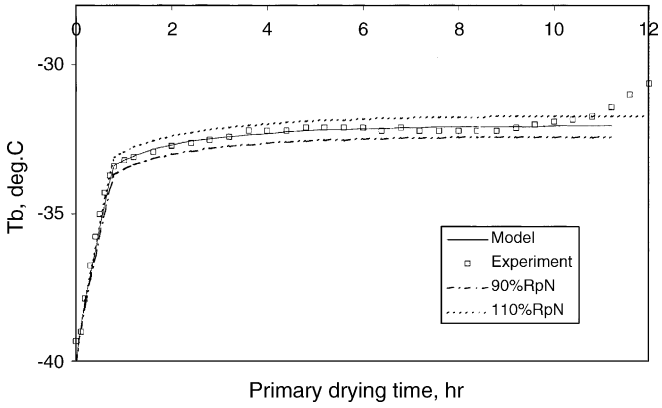

Fig. 7. The experimental and simulated product temperature vs. time profiles for Formulation #5, $R_{pN} = 1.771 + 23.46\ell\square/(1 + 11.62\ell\square)$. The constants and parameters used for the simulation are the same as those of Fig. 4, except R_0, A_1 and A_2.

For the formulations containing sucrose but without mannitol, such as Figs. 6 and 7, the profiles either reached plateau, as shown in Fig. 7, or decreased with time, as shown in Fig. 6. This phenomenon is probably due to the channeling effect in the dry layer or micro-collapse of the matrix, resulting in reduction of the mass transfer resistance when primary drying progresses This can be seen more clearly for Formulation #4 in Fig. 6 where A_1 becomes negative. The negative value of A_1 indicates directly that the resistance at the point probed by the thermocouple decreases with time, and indirectly that the product temperature decreases with time. For this type of T_b profile, the drying time may not be predictable; however, the maximum T_b values can be estimated, so that the primary drying can be maintained below the collapse temperature. It should be noted that the collapse temperature described earlier refers to the "macrocollapse," instead of the micro-collapse of the product. The macroscopic collapse of the matrix during the cycle runs for this formulation was not observed. In fact, after lyophilization Formulation #4 can still maintain the matrix structure, and the cake can be easily reconstituted. In other words, the micro-collapse of the matrix was not due to the cycle parameters. It appears to be a common phenomenon, as observed in our laboratory, of a formulation containing disaccharides such as sucrose, trehalose, and lactose.

4.4. Direct comparison of normalized product resistance

The product resistance values obtained in this work for 3% lactose and 5% mannitol were compared with those in the literature. For 3% lactose–LDH formulation, the closest formulation reported in the literature, with a determined product resistance, is 5% lactose by (Milton et al., 1997, Fig. 8). Milton et al. obtained the resistance using the manometric temperature measurement (MTM) method. For the purpose of reproduce the resistance profile in this figure, the figure was enlarged and the resistance values were estimated and re-plotted in Fig. 9 of this paper. The resistance equation for 3% lactose–LDH formulation obtained in this work is $R_{pN} = 1.771 + 23.46\ell/(1 + 11.62\ell)$, as shown in Table 2, Formulation #5. This equation was also plotted in Fig. 9. It is interesting to see that the two profiles are very close, although the concentrations are different.

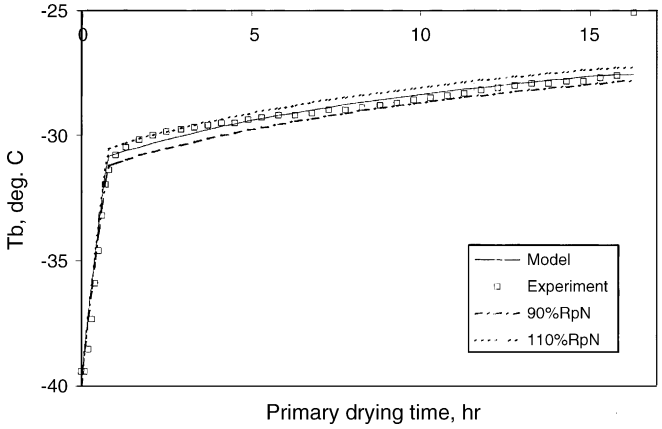

Fig. 8. The experimental and simulated product temperature vs. time profiles for Formulation #6, $R_{pN} = 4.277 + 17.29\ell$. The constants and parameters used for the simulation are the same as those of Fig. 4, except R_0, A_1 and A_2.

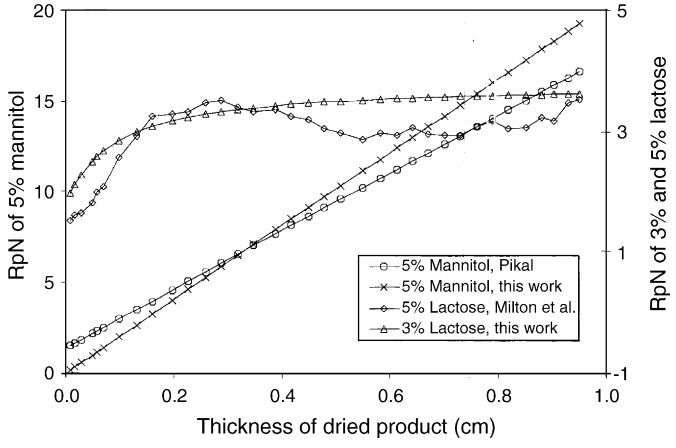

Fig. 9. Direct comparison of the normalized product resistance for 3% lactose and 5% mannitol obtained in this work with those in the literature.

The available product resistance for 5% mannitol in the literature is by (Pikal, 1985, Table 1) obtained by the microbalance method. The obtained resistance expressed by the equation $R_{pN} = 1.40 + 16.0\ell$. The resistance equation obtained in this work is $R_{pN} = 0.0002025 + 20.23\ell$, as indicated in Fig. 4. These two equations are plotted in Fig. 9. It can be seen that the slope of the resistance obtained in this work is slightly higher than that by Pikal. It should be noted that the freezing mechanism of the sample by the microbalance could be different from that of the sample in the vial due to the difference in super-cooling, as described in Section 1. This may result in difference in ice crystal. As such a slight difference in the product resistance could occur.

4.5. Sensitivity of obtained normalized product resistance R_{pN} on the product temperature T_b

The sensitivity was determined by changing the resulting normalized resistance R_{pN}, calculated using the resistance parameters in Table 3, by ±10%, except for 5% mannitol, followed by performing simulation studies using the perturbated resistance to obtain the product temperature profile. The results are presented in Figs. 5–8. For 5% mannitol in Fig. 4, the perturbation of the resistance was set at 20% for easier viewing of the product temperature, since five different profiles are presented together. From the resulting product temperature profiles in Figs. 4–8, it can be seen that a 10% change in the product resistance will result in significantly detectable change in the product temperature profile.

5. Conclusions

Rapid determination for the dry layer product resistance parameters in this paper implies the following. First, vials containing all formulations can be placed on the same shelf and freeze-dried using the same cycle, assuming that the cycle parameters used do not cause collapse. Second, the product temperatures of several vials for each formulation, with a thermocouple in each vial, can be recorded simultaneously. Third, once the simulation (the PDRYS subroutine in Fig. 1) and parameter estimation programs are developed, the product resistance parameters can be determined quickly, using the recorded product temperature profiles I_b.

The computational and experimental results demonstrate that the dry layer product resistance parameters of various pharmaceutical formulations can be rapidly and successfully determined using the proposed approach. This applies to typical T_b profiles (increasing T_b during primary drying), such as those in Figs. 4, 5 and 8, or atypical T_b profiles (plateau-reaching or decreasing T_b during primary drying) such as those in Figs. 6 and 7. With the obtained values of product resistance parameters R_0, A_1 and A_2, various simulations can be performed to determine the maximum product temperature T_b during primary drying. The proposed approach requires only product temperature profiles to be measured and applicable to any laboratory dryer.

Appendix A

Determination of shelf heat transfer coefficient K_s using product temperature profiles and vials with a known heat transfer coefficient K_v

The approach used in this paper for determination of the shelf heat transfer coefficient K_s is based on the two conditions: (1) the product temperature T_b and shelf internal temperature T_f profiles are recorded during the entire course of primary drying and (2) the formulation is lyophilized in vials with previously determined heat transfer coefficient K_v. This approach is similar to that used by Pikal et al. (2005) for determination of the vial heat transfer coefficient K_v.

The theoretical basis for this approach is described below. T_{in}; rate of heat transfer from the shelf internal to the product at the bottom-center of the vial can be obtained by eliminating the shelf surface temperature T_s from Eqs. (22) and (24) (replacing T_t with T_s, since no tray was used in our system) of the paper by Pikal (1985), as given by the following equation:

$$Q = \frac{(T_f - T_b)}{1/(\mathrm{ASV} \cdot K_s) + 1/(A_v K_v)} \tag{A.1}$$

where Q is the heat transfer rate, ASV and A_v are the shelf area per vial and the vial area (calculated based on the outside diameter), respectively. Eq. (A.1) is rearranged to express K_s as a function of other parameters, as

$$\frac{1}{K_s} = \mathrm{ASV}\frac{(T_f - T_b)}{Q} - \frac{\mathrm{ASV}}{A_v K_v} \tag{A.2}$$

Eq. (A.2) indicates that K_s is a function of ASV, A_v, K_v and $(T_f - T_b)/Q$. Eq. (A.2) is applicable to any time interval during primary drying. In Eq. (A.2) the ratio $(T_f - T_b)/Q$ is nearly constant during the entire course of primary drying, since the other parameters K_s, ASV, A_v are constant, and K_v only changes slightly from the beginning to the end of primary drying. The slight change in K_v is due to the variation of the average temperature of T_s and T_b, which affect the radiation coefficient, as described in the text under Section 2.1. Since normally the sublimation rate Q cannot be measured continuously over time, the exact value of the ratio $(T_f - T_b)/Q$ is unknown. However, the average value of $(T_f - T_b)$ during the entire primary drying, denoted as $(T_f - T_b)_{avg}$, can be easily calculated from the recorded data of T_f and T_b. The average sublimation rate during primary drying, denoted as Q_{avg}, can be calculated as equal to the total heat of sublimation divided by the primary drying time. As such, the ratio of the two average values $(T_f - T_b)_{avg}/Q_{avg}$ is obtained. It will be shown later that the calculated ratio $(T_f - T_b)_{avg}/Q_{avg}$ is also approximately equal to the theoretical value of $(T_f - T_b)/Q$ in Eq. (A.2).

In order to obtain K_s from Eq. (A.2), it is required to know the vial heat transfer coefficient K_v which is the sum of three contributions as indicated in Eq. (3) (Pikal, 1985):

$$K_v = K_{cs} + K_r + K_g \tag{A.3}$$

where K_{cs} is the conductive heat transfer coefficient of the contact point between the shelf and glass vial; K_r the radiative heat

Table A.1
Verification of K_s calculations

Assumed K_s (cal s^{-1} cm^{-2} °C^{-1})	Calculated $(T_f - T_b)_{avg}$	Calculated Q_{avg}	Calculated $(T_f - T_b)_{avg}/Q_{avg}$	Theoretical $(T_f - T_b)_{avg}/Q_{avg}$ calculated by Eq. (A.2)	Calculated K_s (cal s^{-1} cm^{-2} °C^{-1})
0.001	12.78	0.02045	624.85	627.56	0.00092
0.002	11.99	0.02274	527.06	531.32	0.0021
0.003	11.68	0.02364	494.39	499.23	0.0032

transfer coefficient, and K_g is the conductive heat transfer coefficient of the gas between the shelf and the glass vial. The radiative heat transfer coefficient K_r is a sum of vial-bottom and vial-top emissivity (e_s and e_v), as expressed by Eq. (4) (Pikal et al., 1984, the coefficient of Eq. (13) in the literature):

$$K_r = 4\sigma\bar{T}^3(e_s + e_v) \tag{A.4}$$

where $\bar{T}$ is the average temperature of the vial bottom T_b and the shelf surface T_s. In order to obtain an accurate value of $4\sigma\bar{T}^3$, it is necessary to know the average temperature $\bar{T}$ over the entire course of primary drying. The value of $4\sigma\bar{T}^3$ appears to be a linear function of the average temperature $\bar{T}$. The value of the coefficient $4\sigma\bar{T}^3$ was calculated as a function of the shelf temperature and product temperature. In order to calculate this value, it is required to perform a primary drying simulation study to generate the temperature profiles of T_b and T_s, based on given information such as the chamber pressure, the set-point of shelf temperature, and the product mass transfer resistance R_{pN}. For the case of a cycle run for mannitol at the shelf temperature of −15 °C and chamber pressure of 100 mTorr (0.1 Torr), the simulated profiles of T_b and T_s were generated from the beginning to the end of primary drying and the values of $4\sigma\bar{T}^3$ was calculated and expressed by the following regression equation:

$$\text{Coeff} = 4\sigma\bar{T}^3 = -0.0001843 + 1.076 \times 10^{-6}\bar{T} \tag{A.5}$$

where the average temperature $\bar{T}$ is in K. For the average temperature of 264.5 and 250 K, the values of Coeff in Eq. (A.5) become 1.00×10^{-4} and 0.847×10^{-4}, respectively.

A.1. Calculated results of K_s using primary drying of 5% mannitol

Since Eq. (A.2) was derived based on theoretical equations, it is independent of the formulation. In order to perform an accurate determination for K_s, it is important to use a formulation that produces accurate and reproducible product temperature profiles, such as 5% mannitol. The glass vial used for lyophilization of 5% mannitol is a Wheaton 10 mL tubing vial, with the fill volume of 3 mL. The product temperature versus time profile T_b is presented in Fig. 4. The two heat transfer parameters, K_{cs} and ℓ_v, obtained by Pikal et al. (1984), are 1.24×10^{-4} cal s^{-1} cm^{-2} °C^{-1} and 0.0471 cm, respectively. The values of ASV and A_v measured by Pikal et al. (1984) are 5.195 and 4.71 cm^2, respectively. The cycle was run using the LyoStar™ II dryer at the chamber pressure of 100 mTorr and the shelf temperature of −15 °C. The temperature profiles of T_f and T_b were recorded, at the time interval of 1 min, for the entire primary drying run. The value of $(T_f - T_b)$ at each time point was calculated. The average value $(T_f - T_b)_{avg}$ was then obtained as equal to 11.97 °C. The primary drying time was estimated to be 1308 min from the average thermocouple reading of five center vials. The average sublimation rate Q_{avg} was calculated as 0.02396 cal s^{-1}. Therefore, the ratio of these two average value $(T_f - T_b)_{avg}/Q_{avg}$ becomes 499.33 °C cal^{-1} s. The vial heat transfer coefficient K_v (calculated by Eqs. (A.3)–(A.5), and Eqs. (5) and (6)) is equal to 5.06×10^{-4} cal s^{-1} cm^{-2} °C^{-1}. Thus, the resulting value of K_s calculated by Eq. (A.2) becomes $K_s = 0.0024$ cal s^{-1} cm^{-2} °C^{-1}.

A.2. Validity of the approach

The validity of the approach described above can be demonstrated by simulation studies of primary drying for 5% mannitol in a 10 mL Wheaton tubing vial. This was accomplished by assuming the shelf set-point T_f at −15 °C, and the chamber pressure at: 100 mTorr, and a shelf transfer coefficient K_s from 0.001 to 0.003 cal s^{-1} cm^{-2} °C^{-1}. The theoretical product temperature profile T_b and the instantaneous sublimation rate Q at each time point were then generated. With these obtained values, the theoretical values of $(T_f - T_b)_{avg}/Q_{avg}$ and K_s can be calculated using the same procedure described above.

The results of calculations are summarized in Table A.1. It can be seen from the table that the calculated values of $(T_f - T_b)_{avg}/Q_{avg}$ are very close to the theoretical values obtained by Eq. (A.2). The resulting calculated K_s values are also very close to those of the assumed ones in the first column of the table. This observation indicates that the approach used in this paper to calculate K_s based on the experimental product temperature profile T_b and the average sublimation rate of primary drying Q_{avg} is appropriate. It should be noted that in order to ensure the resulting value of K_s is accurate, it is important to obtain accurate product temperature profiles and the end point of primary drying.

References

Carnahan, B., Luther, H.A., Wilkes, J.O., 1969. Applied Numerical Methods. John Wiley & Sons Inc., New York.

Dyer, D.F., Sunderland, J.E., 1968. Heat and mass transfer mechanism in sublimation dehydration. J. Heat Trans. 90, 379.

Himmelblau, D.M., 1972. Applied Nonlinear Programming. McGraw-Hill, New York.

Ho, N.F.H., Roseman, T.J., 1979. Lyophilization of pharmaceutical injections: theoretical physical model. J. Pharm. Sci. 68, 1170–1174.

Jennings, T.A., 1988. Discussion of primary drying during lyophilization. J. Parent. Sci. Technol. 42, 118–121.

Karel, M., 1975. Heat and mass transfer in freeze-drying. In: Goldblith, S.A., Rey, L., Rothmayr (Eds.), Freeze-Drying and Advanced Food Technology. Academic Press, New York, pp. 177–202.

Kuester, J.L., Mize, J.H., 1973. Optimization Techniques with FORTRAN. McGraw-Hill, New York, pp. 251–271.

Kuu, W.Y., McShane, J., Wong, J., 1995. Determination of product resistance parameters during freeze drying using modeling and parameter estimation techniques. Int. J. Pharm. 124, 241–252.

Kuu, W.Y., Wood, R.W., Roseman, T.J., 1992. Factors influencing the kinetics of solute release. In: Kydonieus, A. (Ed.), Treatise on Controlled Drug Delivery. Marcel Dekker Inc, New York, pp. 37–154 (Chapter 2).

Lombrana, J.I., Diaz, J.M., 1987. Heat programming to improve efficiency in a batch freeze-drier. Chem. Eng. J. 35, B23–B30.

Mellor, J.D., 1978. Fundamentals of Freeze-Drying. Academic Press, N.Y.

Millman, M.J., Liapis, A.I., Marchello, J.M., 1985. An analysis of the lyophilization process using a sorption-sublimation model and various operational policies. AIChE J. 31, 594–1604.

Milton, N., Pikal, M.J., Roy, M.L., Nail, S.L., 1997. Evaluation of manometric temperature measurement as a method of monitoring product temperature during lyophilization. PDA J. Pharm. Sci. Technol. 51, 7–16.

Nail, S.L., 1980. The effect of chamber pressure on heat transfer in the freeze drying of parenteral solutions. J. Parent. Drug Assoc. 34, 358–368.

Pikal, M.J., Shah, S., Senior, D., Lang, J.E., 1983. Physical chemistry of freeze drying: measurement of sublimation rates for frozen aqueous solutions by a microbalance technique. J. Pharm. Sci. 72, 635–650.

Pikal, M.J., Roy, M.L., Shah, S., 1984. Mass and heat transfer in vial freeze-drying of pharmaceuticals: role of the vial. J. Pharm. Sci. 73, 1224–1237.

Pikal, M.J., 1985. Use of laboratory data in freeze drying process design: heat and product resistance parameters and the compute simulation of freeze drying. J. Parent. Sci. Technol. 39, 115–138.

Pikal, M.J., Cardon, S., Bhugra, C., Jameel, F., Rambhatla, S., Mascarenhas, W.J., Akay, H.U., 2005. The nonsteady state modeling of freeze-drying: in-process product temperature and moisture content mapping and pharmaceutical product quality applications. Pharm. Dev. Technol. 10, 17–32.

Powell, M.D.J., 1965. A method for minimizing a sum of squares of nonlinear functions without calculating derivatives. Comput. J. 7, 303–307.

Tang, X., Nail, S.L., Pikal, M.J., 2005. Freeze-drying process design by manometric temperature measurement: Design of a smart freeze-dryer. Pharm. Res. 22, 685–700.